ISSN: 0975-8585

Research Journal of Pharmaceutical, Biological and Chemical Sciences

A DFT Study of the Inhibition of the Papain-like Protease (PLpro) from the SARS Coronavirus by a Group of 4-Piperidinecarboxamide Derivatives.

Juan S. Gómez-Jeria*.

Quantum Pharmacology Unit, Department of Chemistry, Faculty of Sciences, University of Chile. Las Palmeras 3425, Santiago 7800003, Chile.

ABSTRACT

We present an analysis of the relationships between the electronic structure and the SARS coronavirus papain-like protease inhibitory capacity of a series of 4-piperidinecarboxamide derivatives. The electronic structure of all the molecules was calculated within the Density Functional Theory at the B3LYP/6-31g(d,p) level with full geometry optimization. We found a statistically significant relationship between the variation of the inhibitory capacity and the variation of the values of local atomic reactivity indices pertaining to five atoms of a common skeleton (n=15, adj R^2=0.91, F(5,9)=29.79 (*p<0.00002*), SD=0.24). Molecular electrostatic potentials and conformational aspects of the molecules are discussed. A partial inhibitory pharmacophore is proposed and discussed. This is another example of the needlessness of using hundreds or thousands of reactivity indices and descriptors to get useful physically-based information from experimental results.

Keywords: Papain-like protease, PLpro, SARS, DFT, Coronavirus, QSAR, SAR, Quantum Pharmacology.

Corresponding author

ISSN: 0975-8585

INTRODUCTION

At the end of the year 2002, an outbreak of severe and atypical pneumonia, now called severe acute respiratory syndrome (SARS), was reported in the Guangdong Province of the People's Republic of China. Initially, systemic symptoms of muscle pain, headache and fever were observed. After 2–10 days, the onset of the respiratory symptoms followed (cough, dyspnea, and pneumonia). Severe cases frequently developed quickly, progressing to respiratory distress and requiring intensive care. The epidemics of SARS affected 26 countries, resulting in more than 8,000 cases in 2003. About 9% of SARS-infected patients died (the mortality rate approached 50% for people over 50 years old). Since 2004, there have not been any known cases of SARS. SARS is a viral illness caused by a virus named SARS coronavirus (SARS-CoV) [1-15]. No effective vaccines or antiviral agents have been developed to date. Two targets that seem to be important in the fight against this virus are the SARS-CoV-encoded cisteine proteases, Plpro (papain-like protease) and 3Clpro (chymotrypsin-like protease) [16-21]. The first plays a fundamental role in viral replication and was proposed to be of paramount importance in the pathogenesis of SARS-CoV. Several molecules inhibiting SARS-CoV PLpro have been synthesized and tested [22-45]. Considering the present situation, any approach that could help to understand the inhibitory action of antivirals should be useful. Considering that so far there are no formal quantitative structure-activity relationships studies dealing with antiviral action, we present here the results of a quantum-chemical analysis of the relationships between electronic structure and the *in vitro* SARS-CoV PLpro inhibition for a group of molecules recently synthesized and tested [24].

MATERIALS AND METHODS

Methods

Considering that the methodology employed in this work has solid physical bases that have been presented and discussed in detail in previous works, we present here the final results [46-50]. The logarithm of the biological activity (BA) can be written as:

$$\log(BA)=a+\sum_{j}\left[e_jQ_j+f_jS_j^E+s_jS_j^N\right]+$$

$$+\sum_{j}\sum_{m}\left[h_j(m)F_j(m)+x_j(m)S_j^E(m)\right]+\sum_{j}\sum_{m'}\left[r_j(m')F_j(m')+t_j(m')S_j^N(m')\right]+$$

$$+\sum_{j}\left[g_j\mu_j+k_j\eta_j+o_j\omega_j+z_j\varsigma_j+w_jQ_j^{max}\right]+\sum_{B=1}^{W}O_B \qquad (1)$$

where Q_i is the net charge of atom *i,* S_i^E and S_i^N are the total atomic electrophilic and nucleophilic superdelocalizabilities of Fukui et al., $F_{i,m}$ is the Fukui index of the occupied [empty] molecular orbitals (MO) m [m'] located on atom i. $S_i^E(m)$ is the atomic electrophilic superdelocalizability of MO m on atom i, etc. The total atomic electrophilic superdelocalizability of atom i corresponds to the sum over occupied MOs of all the $S_i^E(m)$'s and the total atomic nucleophilic superdelocalizability of atom i is defined as the sum over empty the MOs of all $S_i^N(m')$'s. The last bracket of Eq. 1 contains new local atomic reactivity indices obtained within the Hartree-Fock-Roothaan framework by an approximate rearrangement of part of the remaining terms of the series expansion employed in our model [46]. The local atomic electronic chemical potential of atom i, μ_i, is defined as:

$$\mu_i=\frac{E_{oc}^*-E_{em}^*}{2} \qquad (2)$$

where E_{oc}^* is the highest occupied MO located on atom with a non-zero Fukui index and E_{em}^* is the lowest vacant MO located on atom i with a non-zero Fukui index. The total local atomic hardness of atom i, η_i, is defined as:

$$\eta_i=E_{em}^*-E_{oc}^* \qquad (3)$$

ISSN: 0975-8585

The total local atomic softness of atom i, ς_i, is defined as the inverse of the local atomic hardness. The local electrophilic index of atom i, ω_i, is defined as:

$$\omega_i = \frac{\mu_i^2}{2\eta_i} \qquad (4)$$

The maximal amount of electronic charge that an electrophile may accept, Q_i^{max}, is defined as:

$$Q_i^{max} = \frac{-\mu_i}{\eta_i} \qquad (5)$$

The physical meaning of these local atomic indices is: μ_i is a measure of the predisposition of an atom to gain or lose electrons; a large negative value indicates a good electron acceptor atom while a small negative value implies a good electron donor atom. η_i is interpreted as the resistance of an atom to exchange electrons with the environment. ω_i is associated with the electrophilic power of an atom and includes the tendency of the electrophile atom to receive extra electronic charge together with its resistance to exchange charge with the medium. The fundamental importance of Eq. 1 is that it contains only terms belonging to the drug molecules.

The moment of inertia term of Eq. 1 can be expressed in a first approximation as [48]:

$$\log\left[(ABC)^{-1/2}\right] = \sum_t \sum_t m_{i,t} R_{i,t}^2 = \sum_t O_t \qquad (6)$$

where the summation is over the different substituents of the molecule, $m_{i,t}$ is the mass of the i-th atom belonging to the t-th substituent, $R_{i,t}$ being its distance to the atom to which the substituent is attached. The physical interpretation of these terms is that they represent the fraction of molecules attaining the proper orientation to interact with the receptor. We have named them Orientation Parameters. Then, for n molecules we have a set of n simultaneous equations 1. This system of simultaneous equations holds for the atoms of the molecule directly concerned in the biological process. These equations can be usefully applied to estimate the relative variation of the biological activities in the family of molecules. This approach has given very good results for a great variety of molecular systems and biological activities [46, 51-73] (and references therein).

Selection of molecules and experimental data

The molecules were selected from a recent study. Their general formula and biological activities are displayed, respectively, in Fig. 1 and Table 2. All the molecules in Fig. 1 have R chirality in the naphthylethyl moiety (marked *). In some molecules the center marked ** has R or S chirality (see Table 1).

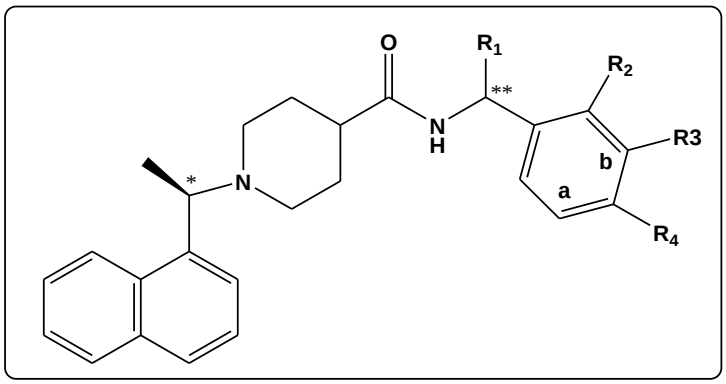

Figure 1: General formulas of 4-piperidinecarboxamide derivatives.

ISSN: 0975-8585

Table 1: 4-piperidinecarboxamide derivatives and SARS-CoV PLpro inhibitory activity.

Mol.	log(IC_{50})	R_1	R_2	R_3	R_4
1	0.34	H	H	H	H
2	1.13	(R)-Me	H	H	H
3	1.10	(S)-Me	H	H	H
4	1.26	(R)-CH_2OMe	H	H	H
5	0.28	(S)-CH_2OMe	H	H	H
6	-0.33	H	H	H	Et
7	-0.22	H	H	H	CONHMe
8	-0.20	H	H	CONHMe	H
9	0.76	H	H	H	NHCOMe
10	-0.41	H	H	NHCOMe	H
11	1.31	H	H	CH_2NHCOMe	H
12	1.43	H	H	Cl	H
13	-0.24	H	H	H	Cl
14	1.31	H	H	F	F
15	-0.31	H	H	H	F
16	-0.82	H	H	F	H
17*	1.42	H	H	------	H
18**	1.26	H	H	H	-----
19**	-0.46	H	OMe	H	-----

* With a N atom at a (Fig. 1). ** With a N atom at b (Fig. 1).

The biological activity selected for this study is the enzyme inhibitory activity of the compounds, expressed as IC_{50} [24].

Calculations

The electronic structure of the molecules was obtained within the Density Functional Theory (DFT) framework at the B3LYP/6-31g(d,p) level after full geometry optimization. The Gaussian suite of programs was used [74]. The values of the LARIs were obtained with the D-CENT-QSAR software [75]. Mulliken Population Analysis results were corrected to avoid negative electron populations [76]. Orientational parameters were calculated as proposed [48]. As it is not possible to solve the system of linear equations because there are not enough molecules, we employed linear multiple regression analysis (LMRA) to discover the local atomic properties implicated in the variation of the biological activity through the series. Statistica software was employed for LMRA [77]. We worked within the hypotheses stating that there is a set of atoms common to all the molecules (called the common skeleton), involved in the biological process. The variation of the numerical values of some local atomic reactivity indices of a number of atoms of the common skeleton accounts for the variation of the biological activity. The substituents modify the electronic structure of the common skeleton and direct the precise alignment of the common skeleton with the papain-like protease site. We built a matrix containing the logarithm of the dependent variable (the enzyme inhibitory activity) and the local atomic reactivity indices of the atoms of the common skeleton as independent variables [75]. The common skeleton numbering is shown in Fig. 2.

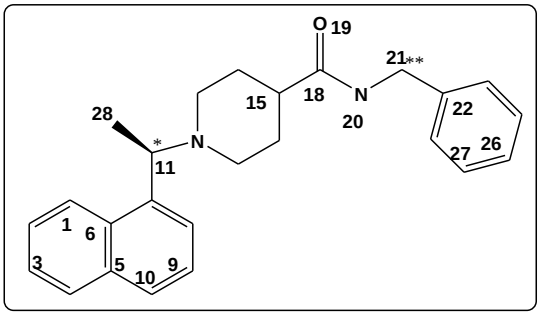

Figure 2: Common skeleton of 4-piperidinecarboxamide derivatives.

ISSN: 0975-8585

RESULTS

The nomenclature employed hereafter is the following. $HOMO_j$* is the highest occupied molecular orbital localized on atom j and $LUMO_j$* is the lowest empty MO localized on atom j. They are called the local atomic frontier MOs. The molecular MOs do not carry an asterisk. The first LMRA for the whole set of molecules (n=19) did not produce any statistically significant equation. Considering that the molecule pairs 2-3 and 4-5 correspond to optical isomers at position 21 (Fig. 2), and that the LARIS's have therefore the same value, we carried out a new LMRA including the orientational effects of the R_1 substituents. No statistically significant equation was obtained. We carried out a new LMRA excluding the optical isomers. After eliminating one outlier, the following equation was obtained:

$$\log(IC_{50}) = 54.02 + 0.40S_{18}^{N}(LUMO)^{*} + 45.04F_{20}(LUMO+2)^{*} - 3.61S_{15}^{N} + \\ + 0.51S_{10}^{N} + 0.43S_{19}^{E}(HOMO-2)^{*} \quad (7)$$

with n=15, R=0.97, R^2=0.94, adj R^2=0.91, F(5,9)=29.79 (*p<0.00002*) and SD=0.24. No outliers were detected and no residuals fall outside the ±2σ limits. Here, $S_{18}^{N}(LUMO)^{*}$ is the local atomic nucleophilic superdelocalizability of the highest occupied MO localized on atom 18, $F_{20}(LUMO+2)^{*}$ is the electron population of the third vacant MO localized on atom 20, S_{15}^{N} is the total atomic nucleophilic superdelocalizability of atom 15, S_{10}^{N} is the total atomic nucleophilic superdelocalizability of atom 10 and $S_{19}^{E}(HOMO-2)^{*}$ is the local atomic electrophilic superdelocalizability of the third highest occupied MO localized on atom 19. Tables 2 and 3 show, respectively, the beta coefficients, the results of the t-test for significance of coefficients and the matrix of squared correlation coefficients for the variables appearing in Eq. 7. Table 3 shows that there are no significant internal correlations between independent variables. Figure 3 shows the plot of observed *vs.* calculated values. The associated statistical parameters of Eq. 7 show that this equation is statistically significant and that the variation of a group of local atomic reactivity indices belonging to the common skeleton explains about 91% of the variation of the inhibitory capacity.

Table 2: Beta coefficients and t-test for significance of coefficients in Eq. 7.

	Beta	t(9)	p-level
$S_{18}^{N}(LUMO)^{*}$	0.61	6.48	<0.0001
$F_{20}(LUMO+2)^{*}$	0.39	4.29	<0.002
S_{15}^{N}	-0.79	-8.07	<0.00002
S_{10}^{N}	0.23	2.73	<0.02
$S_{19}^{E}(HOMO-2)^{*}$	0.56	5.71	<0.0003

Table 3: Matrix of squared correlation coefficients for the variables in Eq. 7.

	$S_{18}^{N}(LUMO)^{*}$	$F_{20}(LUMO+2)^{*}$	S_{15}^{N}	S_{10}^{N}
$F_{20}(LUMO+2)^{*}$	0.30	1.00		
S_{15}^{N}	0.43	0.32	1.00	
S_{10}^{N}	-0.06	-0.17	-0.05	1.00
$S_{19}^{E}(HOMO-2)^{*}$	0.34	-0.11	0.39	0.30

ISSN: 0975-8585

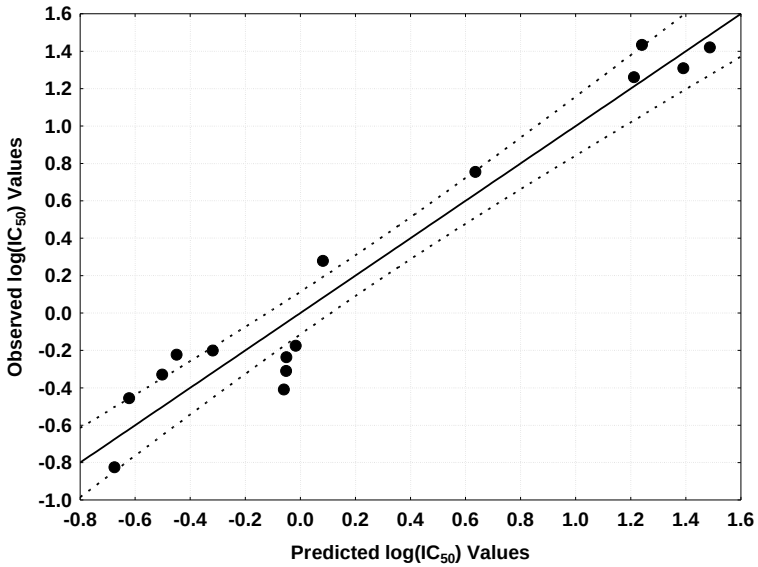

Figure 3: Plot of predicted *vs*. observed log(IC_{50}) values (Eq. 7). Dashed lines denote the 95% confidence interval.

DISCUSSION

Molecular Electrostatic potential (MEP)

For electrostatic forces to be recognized at long distance for subsequent guiding of the molecules toward their action site, we expect some similarity of the MEPs of all molecules. As an example, Fig. 4 shows the MEP maps of molecules 1 and 13 at a distance of 4.5 Å from their nuclei [78].

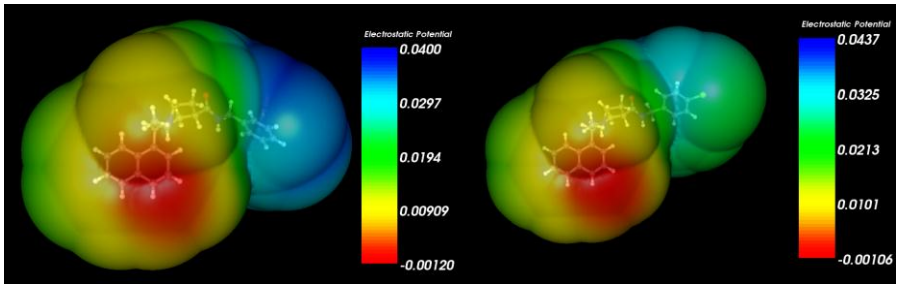

Figure 4: MEP of molecules 1 (left) and 13 (right) at 4.5 Å from the nuclei.

We can see that the MEP maps are very similar: a region of negative MEP exists over one of the faces of the naphthalene moiety while the remainder of the molecule is surrounded by a negative MEP area. Alone, this information is not enough to know which side of the molecule approaches the enzyme. Figure 5 shows the MEP maps of molecules 1 and 13 for an isovalue of ±0.01 [79].

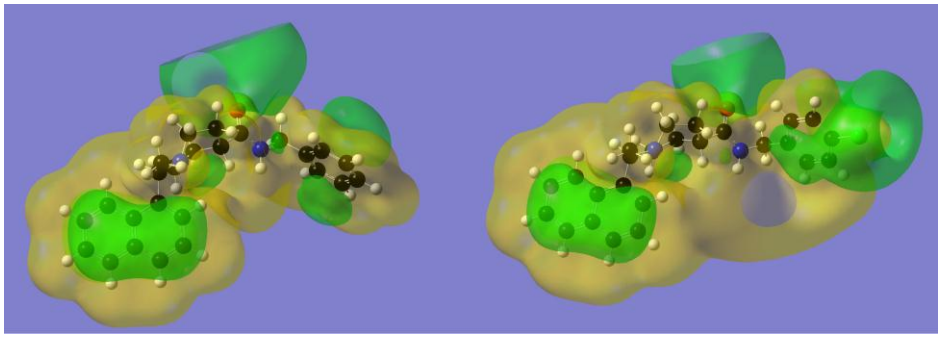

Figure 5. MEP of molecules 1 (left) and 13 (right). The green isovalue surface corresponds to negative MEP values (-0.01) and the yellow isovalue surface to positive MEP values (0.01).

We can see that at shorter distances the MEP maps are similar. Negative MEP areas exist above and below the naphthalene and phenyl moieties and around the oxygen lone pairs. The only difference is that in molecule 13 the chlorine substituent enlarges the negative MEP region of the phenyl substituent.

Conformational aspects

The optimized geometries employed here were obtained for calculations made *in vacuo*. The local atomic reactivity indices produced by these calculations give a good account of several biological phenomena. On the other hand, we cannot expect that the minimum energy conformer will be the same as that found during the experimental measurements. On the basis of only this fact our study assumes implicitly that the numerical value of the LARIs is almost independent of the conformation. There are obvious exceptions, such as the formation of an intramolecular hydrogen bond. As many of biological molecules have a large degree of conformational flexibility it is worth mentioning that in these cases very few experimentalist groups try to restrain the conformational flexibility of the most active compound of the series by using substituents that not significantly alter the electronic structure. Figures 6 and 7 show, respectively, the lowest energy conformers of molecules 1 and 13 obtained with MarvinView software (Dreiding force field) and B3LYP/6-31G** calculations [80].

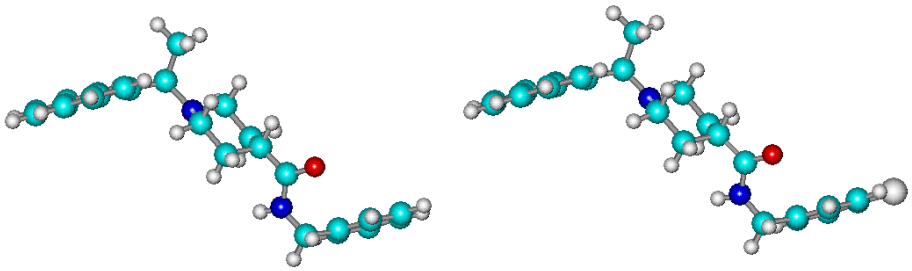

Figure 6: Lowest energy conformers of molecules 1 (left) and 13 (right) (Dreiding force field).

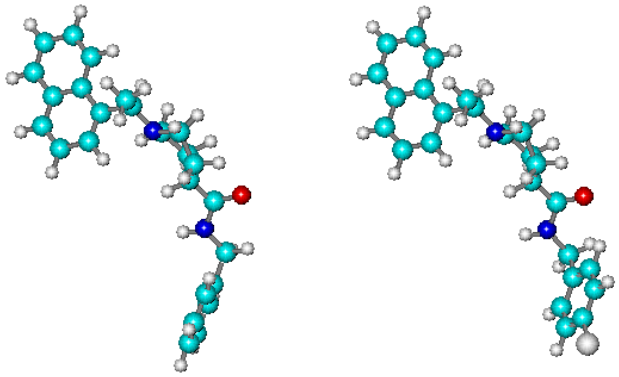

Figure 7: Lowest energy conformers of molecules 1 (left) and 13 (right) (B3LYP/6-31G results).**

We can see that these two methods produce different structures for molecules 1 and 13. We shall take the C(=O)N moiety as a reference point (see Discussion). DFT results show that the naphthalene and phenyl moieties adopt a similar position (Fig. 6). The Dreiding force field results show the same fact (Fig.7). But, if we compare the results for both calculations, we can see that they produce different position for these moieties. Fig. 8 shows the superimposition of B3LYP/6-31G** and Dreiding force field lowest energy conformers of molecules 1 and 13. The C(=O)N moiety was used as the common element for superimposition.

ISSN: 0975-8585

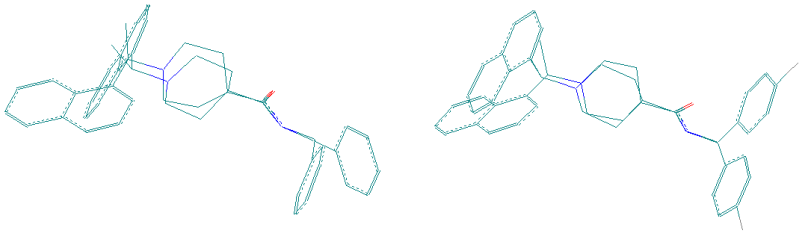

Figure 8: Superimposition of B3LYP/6-31G and Dreiding force field minimum energy conformers for molecules 1 (left) and 13 (right).**

We can see that in both molecules the naphthalene and phenyl moieties are placed in different positions. Anyway, in the experimental situation we face a population of several conformers. The crystallized enzyme-drug data do not help because they represent a frozen situation. Figure 9 shows the ten lowest energy conformers of molecule 1 obtained with MarvinView software and superimposed with Hyperchem [80, 81].

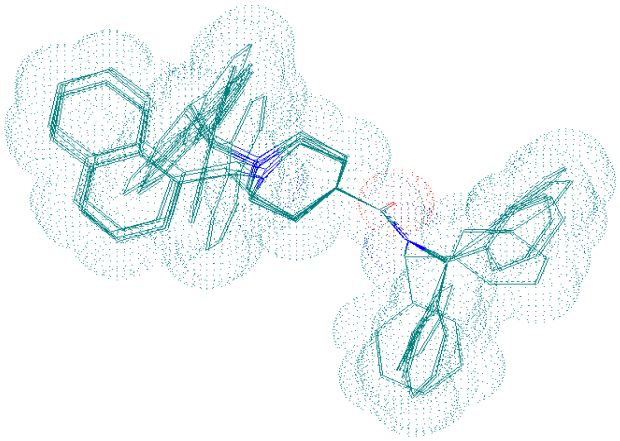

Figure 9: Superimposition of the ten lowest energy conformers of molecule 1.

We can see that the naphthalene and phenyl moieties adopt two main conformations each. Then, instead of using optical isomers at position 11 (all of R chirality in this study, see Fig. 2), it is possible to synthesize conformationally-restricted molecules by substituting position 11 with for example a pair of cyclopropyl, cyclobutyl, *t*-butyl, etc. substituents. In this way molecules with the naphthalene moiety restricted to one position can be obtained and tested. Regarding the phenyl moiety, the same strategy can be employed at C-21 (see Fig. 2). A recent paper on QSAR of PAK1 inhibitors discussed a good example of conformational restriction [60]. Figure 10 shows the ten lowest energy conformers of molecule 13 obtained with MarvinView software and superimposed with Hyperchem [80, 81].

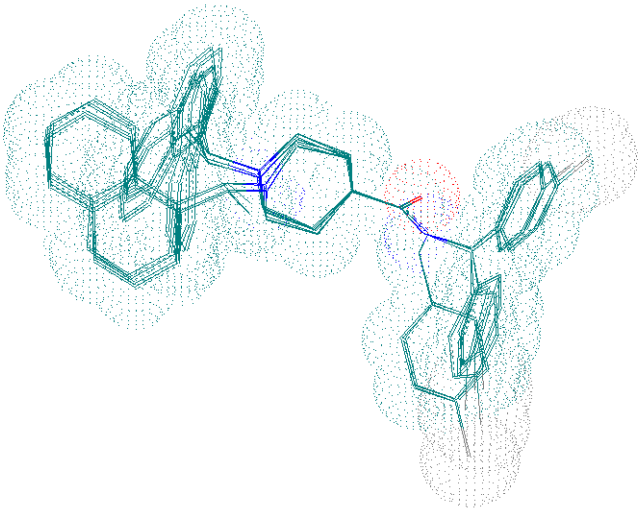

Figure 10: Superimposition of the ten lowest energy conformers of molecule 13.

We can see that we are in the presence of a similar situation as for molecule 1. Therefore, a similar suggestion as above also holds for this case.

Inhibition of SARS-CoV PLpro.

Eq. SSS shows that there is a definite relationship between the variation of the inhibitory capacity and the variation of the values of five local atomic reactivity indices belonging to the common skeleton. The beta values (Table 2) show that the relative importance of these indices is S_{15}^{N} > $S_{18}^{N}(LUMO)^*$ > $S_{19}^{E}(HOMO-2)^*$ > $F_{20}(LUMO+2)^*$ >> S_{10}^{N}.

A variable-by-variable analysis (that is not fully correct) indicates that a high inhibitory capacity is associated with low values for $S_{18}^{N}(LUMO)^*$, $F_{20}(LUMO+2)^*$ and S_{10}^{N}, and with high values for S_{15}^{N} and $S_{19}^{E}(HOMO-2)^*$. The first fact to note is that reactivity indices of atoms 18, 19 and 20, all constituting a C(=O)N system (see Fig. 2), appear in Eq. 7. Therefore, the interpretation of these indices in terms of specific interactions with the enzyme must be carried out keeping internal coherence among them. We present in Table 4 the local MO structure of atoms 18-20.

Table 4: Local Molecular Orbital Structure of Atoms 18-20.

Mol.	Atom 19 (O)	Atom 20 (N)	Atom 18 (C)
2A (100)	93 π94π98π-106π107π109σ	93π94π98π-106π113σ132σ	90σ93π94π-104π105π106π
2B (104)	97π98π102π-107π110σ111σ	97π98π102π-110σ132σ133σ	94π97π98π-107π109π110σ
2C (104)	97π98π102π-107π110σ111σ	97π98π102π-110σ132σ133σ	94π97π98π-107π109π110σ
2D (112)	104π105π106π-118π119π121π	105π106π110π-118π121π137σ	104π105π106π-115π117π118π
2E (112)	104π105π106π-118π119π121π	105π106π110π-118π121π137σ	104π105π106π-115π117π118π
3A (108)	101σ102π106π-114π115π154σ	101σ102π106π-114π119σ125σ	98π101σ102π-112π114π115σ
3B (115)	107σ108π113π-121π122π162σ	108π112π113π-121π127σ152σ	103π107σ108π-120π121π122π
3C (115)	107σ108π113π-121π122π123π	108π109113π-121π130σ145σ	103π107π108π-118π120π121π
3D (115)	108π109π113π-120π121σ122σ	108π109π113π-121σ125σ145σ	106σ107π108π-117π120π121σ
3E (115)	108σ109σ113π-120π121σ122σ	108σ109σ113π-121σ125σ130σ	107σ108σ109σ-117π119π120π
3F (119)	113π116π117π-125σ126π127π	113π116π117π-125σ126π151σ	107π111π112π-123π124π125σ
3G (108)	101σ102σ105π-113π114σ115π	102σ105σ106-114σ115π121σ	97π101σ102σ-110π113π114σ
3H (108)	101π102π106π-113π114σ115π	101π102π106π-114σ115π125σ	97π101π102π-110π113π114σ
3I (108)	101π102π106π-112π113π114σ	101π102π106π-114σ117π126σ	98π101π102π-112π113π114σ
3J (104)	97σ98π102π-110π111σ113π	98π100π102π-110π113π117σ	94π97σ98π-108π109π110π
3K (104)	97σ98π101π-110σ111π113σ	98π101π102-110σ113σ117σ	94π97σ98π-107π108π109π
5A (100)	95π97π98π-105π106π108π	94π95π97π-105π106π128σ	93π94π95π-105π106π107π
5B (100)	94π95π98π-105π106π108π	93σ94π95π-105π106π130σ	92σ93σ94π-105π106π107σ
5C (108)	102π103π105π-113π114π211σ	101σ102π103π-113π114π119σ	101σ102π103π-112π113π114π

Let us consider carbon atom 18 (Fig. 2). The local HOMO* and LUMO* of this atom are energetically far from the molecule's HOMO and LUMO. This strongly suggests that this atom will not act as an electron donor or acceptor. A general tentative role could be related to its ability to facilitate or impede the approach of reactive sites to the adjacent oxygen and/or nitrogen atoms. $LUMO_{18}$* has π nature in all the molecules. A small value for $S_{18}^{N}(LUMO)^*$ can be obtained by an upward shift of the LUMO eigenvalue on the energy axis, by lowering the electron population of the MO or by both procedures. For these reasons we suggest that a low value of $S_{18}^{N}(LUMO)^*$ might facilitate the approach of an atom having one or more vacant MOs by diminishing the repulsive interaction between vacant MOs. This atom seems to belong to a moiety that will also interact with atoms 19 and 20. Atom 20 (nitrogen) also belongs to the C(=O)N system (see Fig. 2). Its first two empty MOs (Table 4) are of ππ, πσ, σπ or σσ character depending on the molecule. A low value of $F_{20}(LUMO+2)^*$, a σ MO in all molecules, suggests that this atom might be interacting with an electron-rich area of the enzyme through its LUMO* and/or (LUMO+1)*. Given the different nature of the first two vacant MOs we suggest that the nitrogen atom might be involved in a hydrogen bond through its H atom. Figs. 4 and 5 show that the MEP area surrounding the N-H system is positive, allowing the approach, for example, of

an oxygen atom to form a H-bond. Oxygen atom 19 is also part of the C(=O)N system. The local $(HOMO-2)_{19}$* is of π nature in all the molecules. A high value for $S_{19}^{E}(HOMO-2)$* is obtained by raising the corresponding electron population, by shifting the MO energy upwards, or by both procedures. As a high value for $S_{19}^{E}(HOMO-2)$* is required, we suggest that atom 20 is interacting with an area of the enzyme having more than one vacant π MO. This suggestion is fully compatible with the requirements for atom 18 and complementary with those for atom 20. A high value for S_{15}^{N}, a carbon atom belonging to a six-membered saturated ring (Fig. 2), is a likely indication that this atom comes close to an electron-rich area of the enzyme (possibly of σ nature). Atom 10 belongs to the naphthalene moiety. The molecular HOMO is localized on this moiety in all the molecules. Then, a low value for S_{10}^{N} could be an indication that this moiety is involved in a π-π stacking interaction, and that atom 10 is facing a center with empty π MOs. All these ideas are represented in the partial two-dimensional (2D) pharmacophore shown in Fig. 11.

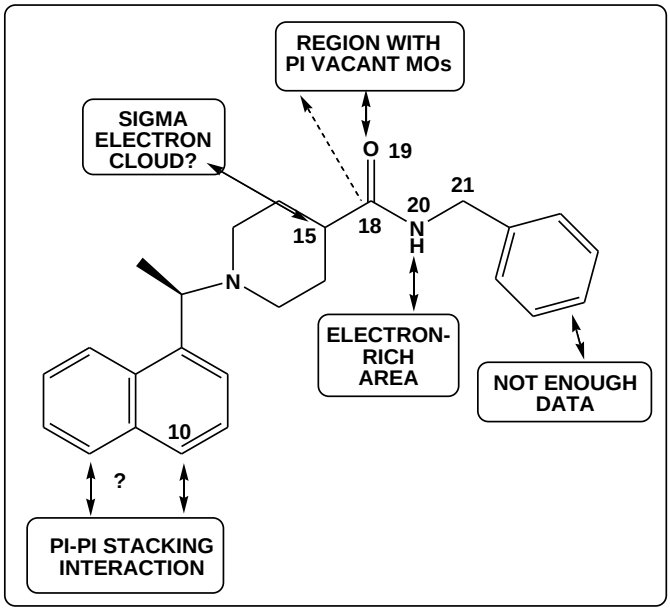

Figure 11: Partial 2D pharmacophore for SARS-CoV PLpro inhibition.

The role of the phenyl moiety remains unclear because no local atomic reactivity indices related to it appear in Eq. 7. It seems that the C(=O)N group plays an important role in the enzyme inhibitory process. Unhappily we do not have a clear explanation for the difference in inhibitory activities of the optical isomers. The problem analyzed here is another example of the needlessness of using hundreds or thousands of reactivity indices and descriptors to get useful information from experimental results.

ACKNOWLEDGEMENTS

Prof. Dr. Bruce K. Cassels (Faculty of Sciences, University of Chile) is thanked for helpful comments.

REFERENCES.

[1] Marra, MA, Jones, SJM, Astell, CR, Holt, RA, Brooks-Wilson, A, Butterfield, YSN, Khattra, J, Asano, JK, Barber, SA, Chan, SY, Cloutier, A, Coughlin, SM, Freeman, D, Girn, N, Griffith, OL, Leach, SR, Mayo, M, McDonald, H, Montgomery, SB, Pandoh, PK, Petrescu, AS, Robertson, AG, Schein, JE, Siddiqui, A, Smailus, DE, Stott, JM, Yang, GS, Plummer, F, Andonov, A, Artsob, H, Bastien, N, Bernard, K, Booth, TF, Bowness, D, Czub, M, Drebot, M, Fernando, L, Flick, R, Garbutt, M, Gray, M, Grolla, A, Jones, S, Feldmann, H, Meyers, A, Kabani, A, Li, Y, Normand, S, Stroher, U, Tipples, GA, Tyler, S, Vogrig, R, Ward, D, Watson, B, Brunham, RC, Krajden, M, Petric, M, Skowronski, DM, Upton, C, Roper, RL. Science, 2003, 300, 1399-1404.

[2] Stanhope, MJ, Brown, JR, Amrine-Madsen, H. Infect. Gen. Evol., 2004, 4, 15-19.

[3] Wang, Z-G, Zheng, Z-H, Shang, L, Li, L-J, Cong, L-M, Feng, M-G, Luo, Y, Cheng, S-Y, Zhang, Y-J, Ru, M-G, Wang, Z-X, Bao, Q-Y. FEBS Lett., 2005, 579, 4928-4936.
[4] Mizutani, T, Fukushi, S, Ishii, K, Sasaki, Y, Kenri, T, Saijo, M, Kanaji, Y, Shirota, K, Kurane, I, Morikawa, S. Biochem. Biophys. Res. Comm., 2006, 347, 261-265.
[5] Shang, L, Qi, Y, Bao, Q-Y, Tian, W, Xu, J-C, Feng, M-G, Yang, H-M. Acta Gen. Sin., 2006, 33, 354-364.
[6] Yuan, J, Yun, H, Lan, W, Wang, W, Sullivan, SG, Jia, S, Bittles, AH. Amer. J. Infect. Contr., 2006, 34, 234-236.
[7] Feng, Y, Gao, GF. Comp. Immun. Microbiol. Infect. Dis., 2007, 30, 309-327.
[8] Tang, JW, Cheung, JLK, Chu, IMT, Ip, M, Hui, M, Peiris, M, Chan, PKS. J. Clin. Virol., 2007, 38, 19-26.
[9] Baric, RS. Virus Res., 2008, 133, 1-3.
[10] Lu, Y, Neo, TL, Liu, DX, Tam, JP. Biochem. Biophys. Res. Comm., 2008, 371, 356-360.
[11] Surjit, M, Lal, SK. Infect. Gen. Evol., 2008, 8, 397-405.
[12] Guo, Y, Tisoncik, J, McReynolds, S, Farzan, M, Prabhakar, BS, Gallagher, T, Rong, L, Caffrey, M. J. Mol. Biol., 2009, 394, 600-605.
[13] Bolles, M, Donaldson, E, Baric, R. Curr. Op. Virol., 2011, 1, 624-634.
[14] Le Gouil, M, Manuguerra, JC. Int. J. Infect. Dis., 2012, 16, Supplement 1, e263.
[15] Kahrstrom, CT. Nat Rev Micro, 2013, 11, 821-821.
[16] Chou, C-Y, Chang, H-C, Hsu, W-C, Lin, T-Z, Lin, C-H, Chang, G-G. Biochem., 2004, 43, 14958-14970.
[17] Huang, C, Wei, P, Fan, K, Liu, Y, Lai, L. Biochem., 2004, 43, 4568-4574.
[18] Kao, RY, To, APC, Ng, LWY, Tsui, WHW, Lee, TSW, Tsoi, H-W, Yuen, K-Y. FEBS Lett., 2004, 576, 325-330.
[19] Han, Y-S, Chang, G-G, Juo, C-G, Lee, H-J, Yeh, S-H, Hsu, JT-A, Chen, X. Biochem., 2005, 44, 10349-10359.
[20] Lindner, HA, Fotouhi-Ardakani, N, Lytvyn, V, Lachance, P, Sulea, T, Ménard, R. J. Virol., 2005, 79, 15199-15208.
[21] Lindner, HA, Lytvyn, V, Qi, H, Lachance, P, Ziomek, E, Ménard, R. Arch. Biochem. Biophys., 2007, 466, 8-14.
[22] Liu, W, Zhu, H-M, Niu, G-J, Shi, E-Z, Chen, J, Sun, B, Chen, W-Q, Zhou, H-G, Yang, C. Bioorg. Med. Chem., 2014, 22, 292-302.
[23] Lee, H, Mittal, A, Patel, K, Gatuz, JL, Truong, L, Torres, J, Mulhearn, DC, Johnson, ME. Bioorg. Med. Chem., 2014, 22, 167-177.
[24] Báez-Santos, YM, Barraza, SJ, Wilson, MW, Agius, MP, Mielech, AM, Davis, NM, Baker, SC, Larsen, SD, Mesecar, AD. J. Med. Chem., 2014, 57, 2393-2412.
[25] Turlington, M, Chun, A, Tomar, S, Eggler, A, Grum-Tokars, V, Jacobs, J, Daniels, JS, Dawson, E, Saldanha, A, Chase, P, Baez-Santos, YM, Lindsley, CW, Hodder, P, Mesecar, AD, Stauffer, SR. Bioorg. Med. Chem. Lett., 2013, 23, 6172-6177.
[26] Thanigaimalai, P, Konno, S, Yamamoto, T, Koiwai, Y, Taguchi, A, Takayama, K, Yakushiji, F, Akaji, K, Kiso, Y, Kawasaki, Y, Chen, S-E, Naser-Tavakolian, A, Schön, A, Freire, E, Hayashi, Y. Eur. J.Med. Chem., 2013, 65, 436-447.
[27] Thanigaimalai, P, Konno, S, Yamamoto, T, Koiwai, Y, Taguchi, A, Takayama, K, Yakushiji, F, Akaji, K, Chen, S-E, Naser-Tavakolian, A, Schön, A, Freire, E, Hayashi, Y. Eur. J.Med. Chem., 2013, 68, 372-384.
[28] Konno, S, Thanigaimalai, P, Yamamoto, T, Nakada, K, Kakiuchi, R, Takayama, K, Yamazaki, Y, Yakushiji, F, Akaji, K, Kiso, Y, Kawasaki, Y, Chen, S-E, Freire, E, Hayashi, Y. Bioorg. Med. Chem., 2013, 21, 412-424.
[29] Jacobs, J, Grum-Tokars, V, Zhou, Y, Turlington, M, Saldanha, SA, Chase, P, Eggler, A, Dawson, ES, Baez-Santos, YM, Tomar, S, Mielech, AM, Baker, SC, Lindsley, CW, Hodder, P, Mesecar, A, Stauffer, SR. J. Med. Chem., 2012, 56, 534-546.
[30] Ryu, YB, Jeong, HJ, Kim, JH, Kim, YM, Park, J-Y, Kim, D, Naguyen, TTH, Park, S-J, Chang, JS, Park, KH, Rho, M-C, Lee, WS. Bioorg. Med. Chem., 2010, 18, 7940-7947.
[31] Ramajayam, R, Tan, K-P, Liu, H-G, Liang, P-H. Bioorg. Med. Chem. Lett., 2010, 20, 3569-3572.
[32] Zhou, Y, Lu, K, Agudelo, J, Simmons, G. Ant. Vir. res., 2009, 82, A37-A38.
[33] Regnier, T, Sarma, D, Hidaka, K, Bacha, U, Freire, E, Hayashi, Y, Kiso, Y. Bioorg. Med. Chem. Lett., 2009, 19, 2722-2727.
[34] Ghosh, AK, Takayama, J, Aubin, Y, Ratia, K, Chaudhuri, R, Baez, Y, Sleeman, K, Coughlin, M, Nichols, DB, Mulhearn, DC, Prabhakar, BS, Baker, SC, Johnson, ME, Mesecar, AD. J. Med. Chem., 2009, 52, 5228-5240.

[35] Shao, Y-M, Yang, W-B, Kuo, T-H, Tsai, K-C, Lin, C-H, Yang, A-S, Liang, P-H, Wong, C-H. Bioorg. Med. Chem., 2008, 16, 4652-4660.
[36] Nukoolkarn, V, Lee, VS, Malaisree, M, Aruksakulwong, O, Hannongbua, S. J. Theor. Biol., 2008, 254, 861-867.
[37] Niu, C, Yin, J, Zhang, J, Vederas, JC, James, MNG. Bioorg. Med. Chem., 2008, 16, 293-302.
[38] Ghosh, AK, Gong, G, Grum-Tokars, V, Mulhearn, DC, Baker, SC, Coughlin, M, Prabhakar, BS, Sleeman, K, Johnson, ME, Mesecar, AD. Bioorg. Med. Chem. Lett., 2008, 18, 5684-5688.
[39] Ikejiri, M, Saijo, M, Morikawa, S, Fukushi, S, Mizutani, T, Kurane, I, Maruyama, T. Bioorg. Med. Chem. Lett., 2007, 17, 2470-2473.
[40] Hu, D, Shao, C, Guan, W, Su, Z, Sun, J. J. Inorg. Biochem., 2007, 101, 89-94.
[41] Ghosh, AK, Xi, K, Grum-Tokars, V, Xu, X, Ratia, K, Fu, W, Houser, KV, Baker, SC, Johnson, ME, Mesecar, AD. Bioorg. Med. Chem. Lett., 2007, 17, 5876-5880.
[42] Yang, S, Chen, S-J, Hsu, M-F, Wu, J-D, Tseng, C-TK, Liu, Y-F, Chen, H-C, Kuo, C-W, Wu, C-S, Chang, L-W, Chen, W-C, Liao, S-Y, Chang, T-Y, Hung, H-H, Shr, H-L, Liu, C-Y, Huang, Y-A, Chang, L-Y, Hsu, J-C, Peters, CJ, Wang, AHJ, Hsu, M-C. J. Med. Chem., 2006, 49, 4971-4980.
[43] Sydnes, MO, Hayashi, Y, Sharma, VK, Hamada, T, Bacha, U, Barrila, J, Freire, E, Kiso, Y. Tetrahed., 2006, 62, 8601-8609.
[44] Lu, IL, Mahindroo, N, Liang, P-H, Peng, Y-H, Kuo, C-J, Tsai, K-C, Hsieh, H-P, Chao, Y-S, Wu, S-Y. J. Med. Chem., 2006, 49, 5154-5161.
[45] Ho, T-Y, Wu, S-L, Chen, J-C, Wei, Y-C, Cheng, S-E, Chang, Y-H, Liu, H-J, Hsiang, C-Y. Ant. Vir. res., 2006, 69, 70-76.
[46] Gómez-Jeria, JS. Canad. Chem. Trans., 2013, 1, 25-55.
[47] Gómez-Jeria, JS, *Elements of Molecular Electronic Pharmacology (in Spanish),* Ediciones Sokar, Santiago de Chile, 2013.
[48] Gómez-Jeria, JS, Ojeda-Vergara, M. J. Chil. Chem. Soc., 2003, 48, 119-124.
[49] Gómez-Jeria, JS, "Modeling the Drug-Receptor Interaction in Quantum Pharmacology," in *Molecules in Physics, Chemistry, and Biology*, J. Maruani Ed., vol. 4, pp. 215-231, Springer Netherlands, 1989.
[50] Gómez-Jeria, JS. Int. J. Quant. Chem., 1983, 23, 1969-1972.
[51] Solís-Gutiérrez, R, Gómez-Jeria, JS. Res. J. Pharmac. Biol. Chem. Sci., 2014, 5, 1401-1416.
[52] Salgado-Valdés, F, Gómez-Jeria, JS. J. Quant. Chem., 2014, 2014 Article ID 431432, 1-15.
[53] Pino-Ramírez, DI, Gómez-Jeria, JS. Amer. Chem. Sci. J., 2014, 4, 554-575.
[54] Muñoz-Gacitúa, D, Gómez-Jeria, JS. J. Comput. Methods Drug Des., 2014, 4, 48-63.
[55] Muñoz-Gacitúa, D, Gómez-Jeria, JS. J. Comput. Methods Drug Des., 2014, 4, 33-47.
[56] Gómez-Jeria, JS, Molina-Hidalgo, J. J. Comput. Methods Drug Des., 2014, 4, 1-9.
[57] Gómez-Jeria, JS. J. Comput. Methods Drug Des., 2014, 4, 32-44.
[58] Gómez-Jeria, JS. Res. J. Pharmac. Biol. Chem. Sci., 2014, 5, 2124-2142.
[59] Gómez-Jeria, JS. Der Pharma Chem., 2014, 6, 64-77.
[60] Gómez-Jeria, JS. SOP Trans. Phys. Chem., 2014, 1, 10-28.
[61] Gómez-Jeria, JS. Brit. Microbiol. Res. J., 2014, 4, 968-987.
[62] Gómez-Jeria, JS. Der Pharm. Lett., 2014, 6., 95-104.
[63] Gómez-Jeria, JS. Int. Res. J. Pure App. Chem., 2014, 4, 270-291.
[64] Reyes-Díaz, I, Gómez-Jeria, JS. J. Comput. Methods Drug Des., 2013, 3, 11-21.
[65] Paz de la Vega, A, Alarcón, DA, Gómez-Jeria, JS. J. Chil. Chem. Soc., 2013, 58, 1842-1851.
[66] Gómez-Jeria, JS, Flores-Catalán, M. Canad. Chem. Trans., 2013, 1, 215-237.
[67] Alarcón, DA, Gatica-Díaz, F, Gómez-Jeria, JS. J. Chil. Chem. Soc., 2013, 58, 1651-1659.
[68] Bruna-Larenas, T, Gómez-Jeria, JS. Int. J. Med. Chem., 2012, 2012 Article ID 682495, 1-16.
[69] Barahona-Urbina, C, Nuñez-Gonzalez, S, Gómez-Jeria, JS. J. Chil. Chem. Soc., 2012, 57, 1497-1503.
[70] Gómez-Jeria, JS. J. Chil. Chem. Soc., 2010, 55, 381-384.
[71] Gómez-Jeria, JS, Morales-Lagos, D, Rodriguez-Gatica, JI, Saavedra-Aguilar, JC. Int. J. Quant. Chem., 1985, 28, 421-428.
[72] Gómez-Jeria, JS, Morales-Lagos, DR. J. Pharm. Sci., 1984, 73, 1725-1728.
[73] Gómez-Jeria, JS, Morales-Lagos, D, "The mode of binding of phenylalkylamines to the Serotonergic Receptor," in *QSAR in design of Bioactive Drugs*, M. Kuchar Ed., pp. 145-173, Prous, J.R., Barcelona, Spain, 1984.
[74] Frisch, MJ, Trucks, GW, Schlegel, HB, Scuseria, GE, Robb, MA, Cheeseman, JR, Montgomery, J, J.A., Vreven, T, Kudin, KN, Burant, JC, Millam, JM, Iyengar, SS, Tomasi, J, Barone, V, Mennucci, B, Cossi, M, Scalmani, G, Rega, N. Gaussian98 Rev. A.11.3, Gaussian, Pittsburgh, PA, USA, 2002.

[75] Gómez-Jeria, JS. D-Cent-QSAR: A program to generate Local Atomic Reactivity Indices from Gaussian log files. 1.0, Santiago, Chile, 2014.
[76] Gómez-Jeria, JS. J. Chil. Chem. Soc., 2009, 54, 482-485.
[77] Statsoft. Statistica 8.0, 2300 East 14 th St. Tulsa, OK 74104, USA, 1984-2007.
[78] Varetto, U. Molekel 5.4.0.8, Swiss National Supercomputing Centre: Lugano, Switzerland, 2008.
[79] Dennington, RD, Keith, TA, Millam, JM. GaussViev 5.0.8, 340 Quinnipiac St., Bldg. 40, Wallingford, CT 06492, USA, 2000-2008.
[80] Chemaxon. MarvinView, www.chemaxon.com, USA, 2014.
[81] Hypercube. Hyperchem 7.01, 419 Phillip St., Waterloo, Ontario, Canada, 2002.